Parametric instabilities of phonons: Nonlinear infrared absorption*

M. Sparks
Xonics, Incorporated, 6849 Hayvenhurst Avenue, Van Nuys, California 91406

H. C. Chow
Department of Physics, University of California, Los Angeles, California 90024
and Xonics, Incorporated, 6849 Hayvenhurst Avenue, Van Nuys, California 91406

(Received 4 March 1974)

Nonlinear infrared absorption by parametric phonon processes is shown to be negligible in the low-absorption region of exponential frequency dependence of the optical-absorption coefficient β, but observable at the reststrahl resonance and in Raman scattering. At low intensity, the transmission T is independent of intensity I as usual, but at high intensity the $T(\omega)$ curve broadens and the transmission at resonance increases. This behavior results from the parametric instability in the process in which an intermediate-state reststrahl phonon is annihilated and a pair of phonons is created. An effective relaxation frequency of the reststrahl phonon, which is greater than the low-intensity value as a result of the increase in the amplitudes of the pair phonons above their thermal equilibrium values, is quite useful in understanding absorption and Raman-scattering results. The time constant for the approach to the steady state is important since the steady state is not attained in short laser pulses in important cases in which long-lived phonons give rise to low steady-state threshold intensities for anomalous absorption. The threshold for the parametric instability is quite sharp when considered as a function of the *amplitude of the fundamental phonon*, but the deviation from linear absorption with increasing *intensity* is quite smooth. Contrary to previously accepted results, even crystals such as NaCl having a center of inversion could have anomalously low thresholds since the threshold is controlled by the phonon (in the pair) having the longer lifetime. Chain instabilities and enhanced relaxation from mutual interaction of excited pair phonons are negligible for the phonon instabilities, in contrast to previous results for plasmas and parallel pumping in ferromagnetic resonance, respectively. The method of calculation, using boson occupation numbers rather than mode amplitudes, has the simplicity and power to yield more information about parametric instabilities, including effects above the threshold, than has been possible previously.

I. INTRODUCTION

Parametric processes are well known in ferromagnetic resonance,[1-4] plasma physics,[5,6] nonlinear optics, especially stimulated Raman and Brillouin scattering,[7] and many electrical devices.[8] However, apart from Orbach's work showing that it should be possible to create large numbers of long-lifetime phonons on the lowest transverse-optical branch by a parametric instability,[9] there apparently have been no studies of phonon instabilities. In particular, the effect of parametric instabilities of phonons on optical absorption has not been considered in spite of considerable interest in nonlinear optical effects.

Since the parametric instabilities typically occur at high laser intensities, there are a number of high-intensity effects that could mask the parametric effects. These include absorption by macroscopic inclusions,[10-12] avalanche breakdown,[10,13] self-focusing effects,[14] and differential heating by linear abosrption.[15] In previous calculations, the instability threshold for an isolated process, such as annihilation of one boson and the creation of two other bosons, has been obtained simply from linearized equations of motion of the mode amplitudes or the mode occupation numbers. More detailed calculations have been severely hampered by the complexity of the nonlinear mode-amplitude equations, especially near and above the threshold, and the difficulty introduced by requiring the amplitudes to relax to their thermal equilibrium values.[1]

In the present paper, the nonlinear absorption of infrared radiation by parametric excitation of phonons is considered and a general method of solving parametric problems is presented. As discussed in Sec. II A, an example of a process that has a parametric instability is shown in Fig. 1, where the intermediate phonon f is a fundamental, or reststrahl phonon (transverse-optical mode with wavelength $k \cong 0$). Special attention is focused on ionic crystals such as NaCl, though the discussion for the most part is quite general. Absorption, as opposed to scattering, processes are emphasized. The results of a similar study on the effect of parametric instabilities of phonons on stimulated Raman scattering and on the parametric instability in the Raman process itself[16] will be presented elsewhere.[17]

The present treatment differs from previous ones in the following ways: (a) consideration of the nonlinear effects of phonon instabilities on infrared absorption; (b) treatment of transient, as well as steady-state, effects; (c) development of a

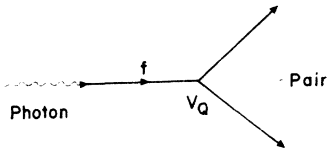

FIG. 1. Two-phonon processes.

simple method of calculation which is used even above the threshold; (d) incorporation of effects of sums over potentially unstable modes; (e) analysis of chain parametric processes and enhanced relaxation of output phonons; (f) treatment of the instability in the Lax-Burstein higher-order-dipole-moment process; and (g) consideration of processes in which two fundamental phonons are annihilated.

The following results are obtained: (a) prediction that the thin-film infrared transmission spectrum $T(\omega)$ of crystals is independent of intensity I at low I as usual, but that for $I \gtrsim \frac{1}{2} I_c$, where I_c is the critical intensity for the parametric threshold, the reststrahl resonance in $T(\omega)$ broadens and the transmission at resonance increases with increasing I; (b) calculation of the value of I_c showing that at the reststrahl resonance I_c can range from $\sim 10^{-7}$ to 10^{11} W/cm^2; (c) demonstration that the nonlinear parametric-phonon-instability absorption in the infrared region of low multiphonon absorption is negligible with respect to the electron avalanche-breakdown process; (d) indication that transient effects are important, especially in rendering unobservable by present short-pulse lasers the low thresholds resulting from ultralong-lifetime phonons[9]; (e) demonstration that the instability threshold is sharp when considered as a function of the amplitude n_f of the intermediate (fundamental) phonon, but is a smooth function of the laser intensity I; (f) analysis of effects of many potentially unstable modes which evinces that the value of n_f is considerably less than its threshold value n_c even when $I \gg I_c$; (g) calculation of an effective relaxation frequency $\tilde{\Gamma}_f$ for the intermediate mode which shows that $\tilde{\Gamma}_f$ is greater than the usual linear, low-intensity value Γ_f as a result of the increase in the amplitudes n_Q of the output phonons responsible for the damping Γ_f; (h) indication that even crystals (such as NaCl-structure crystals) having a center of inversion could have anomalously low thresholds I_c, since the threshold is controlled by the output phonon having the longer lifetime when the two phonons are on different branches; (i) derivation of simple closed-form expressions for transmissivity as a function of I, for $n_f(I)$, for $\tilde{\Gamma}_f(n_f)$, and for $\tilde{\Gamma}_f(I)$; (j) calculation of I_c for n-phonon processes with $n > 2$, which shows that these nonlinear higher-order processes are negligible; (k) analysis of chain parametric-instability processes, indicating that these phonon processes are negligible, in contrast to the cases of ferromagnetic resonance and plasma instabilities; and (l) calculation of I_c for the process in which two reststrahl phonons are annihilated and two other phonons are created, which shows that this process may be important in some cases.

Significant results will be denoted by underscored equation numbers.

II. TWO-PHONON INSTABILITY

A. Physical description

In this section a simple physical description of the two-phonon parametric instability will be given. Consider the two-phonon process in which a photon is annihilated, a fundamental phonon is created, then annihilated, and two other phonons are created, as illustrated in Fig. 1.[18] This process is directly analogous to the Bloch-Bloembergen-Suhl subsidiary-resonance process which occurs at high power levels in ferromagnetic resonance. The fundamental phonon corresponds to the uniform precession magnon (with $\vec{k} = 0$) and the pair of created phonons corresponds to a pair of created magnons.[19]

The present section concerns the part of the process in Fig. 1 in which one phonon splits into two phonons, called the pair. The analysis applies to other cases also. For example, the fundamental phonon could be created in the Raman-Stokes process.

The two-phonon process gives rise to ordinary linear absorption at low power levels.[20] In that case, the relaxation of the pair phonons maintains their occupation numbers n_Q at their thermal equilibrium values $\bar{n}_Q$. At higher power levels, n_Q increases above $\bar{n}_Q$. As the intensity I of the radiation increases, the fundamental-mode amplitude n_f increases, and in turn the amplitude of the output pair increases. The balance of power into the pair from the fundamental mode by the power out of the pair by relaxation is the first key to a simple explanation of the parametric instability. The power into the pair increases nonlinearly; that is, the power contains products such as $2n_f n_Q$, since the second vertex in Fig. 1 involves three phonons. On the other hand, the power out of the pair by relaxation increases linearly as $2\Gamma(n_Q - \bar{n}_Q)$, where Γ is the relaxation frequency of an output phonon. Thus, at a critical value n_c of n_f, the amplitude n_Q becomes very large.

This behavior is analogous to that of a pendulum with a force having frequency $\omega = 2\omega_r$, where ω_r is the resonant frequency of the pendulum, applied along the direction of gravity: For a small angle θ, the loss is linear in θ, while the energy that the force puts into the pendulum (the scalar product of force and distance) is proportional to θ^2, since the

projection of the motion along the vertical is proportional to θ^2. The pendulum instability is discussed further in Ref. 21. The details of this type of behavior will now be discussed.

B. Instability threshold of a pair

The threshold value n_c of n_f at the parametric-instability threshold and the increase of the pair-mode occupation number n_Q as n_f increases will now be derived, and it will be shown that n_Q increases extremely rapidly as n_f approaches and slightly exceeds n_c, as will be seen in Fig. 2 below.

First consider the power flow from the fundamental mode to the potentially unstable pair in Fig. 1. The Hamiltonian for this process (vertex V_Q in the figure) is[20,22]

$$\mathcal{H} = \sum_{Q_1 Q_2 Q_3} \hbar V_{Q_1 Q_2 Q_3} A_{Q_1} A_{Q_2} A_{Q_3} , \tag{2.1}$$

where $Q_i \equiv (\vec{k}_i, b_i)$ specifies the phonon mode with wave vector $\vec{k}_i$ on branch b_i, $A_{Q_i} \equiv a^\dagger_{Q_i} + a_{-Q_i}$ [with $-Q_i \equiv (-\vec{k}_i, b_i)$], and $a^\dagger$ and a are the usual phonon creation and annihilation operators normalized to unit commutators. From the standard second-order perturbation-theory result for the transition probability between the states of a system, the rate of change of n_f resulting from the coupling to a single pair of phonons Q_1 and Q_2 is[4]

$$\frac{dn_f}{dt} = \frac{2\pi}{\hbar^2} \left\{ \left| \langle n_f + 1, n_{Q_1} - 1, n_{Q_2} - 1 \left| \mathcal{H} \right| n_f, n_{Q_1}, n_{Q_2} \rangle \right|^2 - \left| \langle n_f - 1, n_{Q_1} + 1, n_{Q_2} + 1 \left| \mathcal{H} \right| n_f, n_{Q_1}, n_{Q_2} \rangle \right|^2 \right\} \delta(\tilde{\omega}) , \tag{2.2}$$

where δ is the Dirac δ function and $\tilde{\omega} \equiv \omega - \omega_{Q_1} - \omega_{Q_2}$, with ω the frequency of the photon.

In detailed calculations for specific cases it is important to consider the case of unequal frequencies ω_{Q_1} and ω_{Q_2} since in NaCl-structure crystals a selection rule[23-26] prohibits both phonons of the pair from being on the same branch and a quasi-selection rule[27] indicates that the coupling of a fundamental phonon to two acoustical or to two optical phonons is small. However, no essential features of the calculation are lost in the case of equal frequencies and equal relaxation frequencies Γ_Q. The presentation will therefore be simplified by formally using these approximations. The case of $\omega_{Q_1} \neq \omega_{Q_2}$ and $\Gamma_{Q_1} \neq \Gamma_{Q_2}$ is considered in Sec. II D. The occupation numbers n_Q of the two phonons in the pair are equal since $\bar{n}_{Q_1} = \bar{n}_{Q_2}$, where the bar denotes the thermal-equilibrium value as before, the two-phonon process creates the phonons in equal numbers, and $\Gamma_{Q_1} = \Gamma_{Q_2}$.

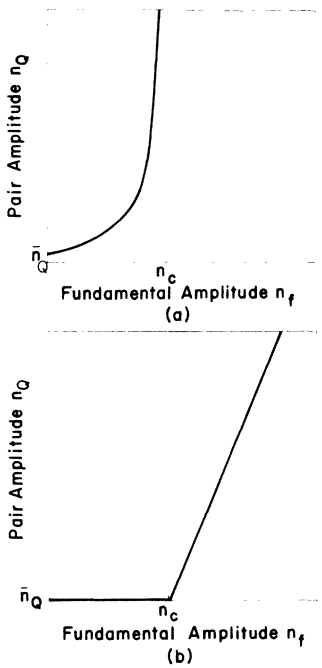

FIG. 2. Increase of the pair amplitude with increasing n_f. (a) The ordinate scale is such that $\bar{n}_Q$ is visible. (b) The ordinate scale is many orders of magnitude smaller than (a).

Substituting Eq. (2.1) into (2.2), using the fact that $V_{f Q_1 Q_2}$ vanishes unless $\vec{k}_1 = -\vec{k}_2$, and using the well-known matrix elements of $a^\dagger$ and a gives

$$\left(\frac{dn_Q}{dt}\right)_{\text{pump}} = C\tilde{n} , \tag{2.3}$$

where

$$\tilde{n} = 2n_f n_Q + n_f - n_Q^2, \quad C = \pi \left| 3! V_{f Q -Q} \right|^2 \delta(\tilde{\omega}) . \tag{2.4}$$

The subscript "pump" in Eq. (2.3) denotes the rate of change of n_Q from the coupling to f. The energy-conserving δ function will be eliminated by taking into account the finite lifetime of the pair, as discussed below.

In equilibrium, the net rate of change of n_Q must be zero. Thus, the rate of increase in Eq. (2.3) is added to the rate of decrease by relaxation

$$\left(\frac{dn_Q}{dt}\right)_{\text{relax}} = -\Gamma_Q (n_Q - \bar{n}_Q) , \tag{2.5}$$

and the result is set equal to zero to obtain

$$2n_f n_Q + n_f - n_Q^2 = 2n_c (n_Q - \bar{n}_Q), \quad n_c \equiv \Gamma_Q / 2C . \tag{2.6}$$

The solution to (2.6) is

$$n_Q = (n_c - n_f) \left[\operatorname{sgn}(n_c - n_f) \left(1 + \frac{2n_c \bar{n}_Q + n_f}{(n_c - n_f)^2} \right)^{1/2} - 1 \right] , \tag{2.7}$$

where $\mathrm{sgn}x \equiv +1$ for $x > 0$ and -1 for $x < 0$. Equation (2.7) has the limiting values:

$$n_Q \cong \bar{n}_Q, \qquad \text{for } n_f \ll n_c \qquad (2.8a)$$

$$n_Q = [n_c(2\bar{n}_Q + 1)]^{1/2}, \qquad \text{for } n_f = n_c \qquad (2.8b)$$

and

$$n_Q \cong 2(n_f - n_c), \qquad \text{for } n_f \gg n_c, \qquad (2.8c)$$

as sketched in Fig. 2. We shall say that the pair has been driven *unstable* if $n_Q \geq [n_c(2\bar{n}_Q + 1)]^{1/2}$, or $n_f \geq n_c$, and the *threshold* of the instability is defined by $n_f = n_c$. At the critical value n_c of n_f there is a sharp dramatic increase in the value of n_Q. The sharpness is illustrated by considering values of n_Q slightly below and slightly above the threshold. At $n_f = n_c - \epsilon n_c$, where $[(2\bar{n}_Q + 1)/n_c]^{1/2} \ll \epsilon \ll 1$, Eq. (2.7) gives $n_Q \cong (\bar{n}_Q + \frac{1}{2})/\epsilon$, which is of order 10^3 for $\bar{n}_Q \lesssim 1$ and $\epsilon = 10^{-3}$. At $n_f = n_c + \epsilon n_c$, Eq. (2.7) gives $n_Q = 2\epsilon n_c$, which is order 10^{19} for $\epsilon = 10^{-3}$ and $n_c = 10^{22}$; i.e., n_Q increases by 16 orders of magnitude for a small change of n_f at $n_f \cong n_c$.

The behavior below the threshold was approximated previously[3,4] for the ferromagnetic-resonance case by linearizing the equation of motion. In the present case, linearizing Eq. (2.6) by neglecting the term $-n_Q^2$ gives

$$n_Q = \frac{\bar{n}_Q + n_f/2n_c}{1 - n_f/n_c}, \qquad (2.9)$$

which displays the instability at $n_f = n_c$ vividly, since $n_Q \to \infty$ there. On a linear scale with $\bar{n}_Q$ visible, a graph of n_Q from (2.7) would have the appearance of Eq. (2.9), since n_Q would be off scale at a value of n_f less than n_c according to the discussion in the previous paragraph. It will be shown in Sec. III B that the large number of potentially unstable pairs in the present case of phonons restricts n_f to values below $n_f - \epsilon$, so that Eq. (2.9) is a good approximation in all cases of interest here.

Next, consider the value of n_c in Eq. (2.6). An estimate of the size of the matrix element V_{fQ-Q} in Eq. (2.4) is obtained simply[4] by summing the right-hand side of Eq. (2.2) over $Q \equiv Q_1 = -Q_2$, assuming that $n_Q = \bar{n}_Q$ and $n_{-Q} = \bar{n}_{-Q}$, evaluating the sum on Q by assuming a Debye density of states, and approximating the Debye frequency by ω_f. This gives

$$|3!\, V_{fQ-Q}|^2 N = S_Q \omega_f \Gamma_f / (2\bar{n}_Q + 1)p, \qquad (2.10)$$

where N is the number of unit cells in the sample and p is the number of pairs of branches into which the fundamental phonon decays. For example, $p < 6 + 5 + \cdots + 1 = 21$ for a solid with six branches, and $p = 3 + 2 + 1 = 6$ for decay into acoustical modes in diamond. The factor S_Q, which was added formally to Eq. (2.10) to account for the variation of V_{fQ-Q} with Q, is zero for transitions not allowed by symmetry,[23-26] is much less than unity for quasiunallowed transitions,[27] and is of order unity for fully allowed transitions. An alternate expression for V_{fQ-Q} is given below in Eq. (2.24).

In Eq. (2.4), the δ function $\delta(\tilde{\omega})$ is appropriate when a sum (approximated by an integral) is involved. In the present case no sum is involved since the energy into a single pair is of interest. Thus, following Callen[2] and White and Sparks,[3] the δ function is replaced by a normalized line-shape factor

$$\delta(\omega - 2\omega_Q) \to \frac{2}{\pi} \frac{\omega(2\omega_Q)(2\Gamma_Q)}{[\omega^2 - (2\omega_Q)^2]^2 + (2\omega_Q)^2(2\Gamma_Q)^2} \cong \frac{1}{\pi\Gamma_Q}, \qquad (2.11)$$

where the approximate equality is valid at resonance ($\omega = 2\omega_Q$). Substituting Eqs. (2.11), (2.10), and (2.4) into (2.6) gives

$$\frac{n_c}{N} \cong \frac{p(2\bar{n}_Q + 1)[(\omega^2 - 4\omega_Q^2)^2 + 16\omega_Q^2\Gamma_Q^2]}{16 S_Q \omega \omega_Q \omega_f \Gamma_f}. \qquad (2.12)$$

The resonant value of n_c is denoted n_p. From Eq. (2.12) with $\omega = 2\omega_Q$,

$$\frac{n_p}{N} \cong \frac{p(\bar{n}_Q + \frac{1}{2})\Gamma_Q^2}{S_Q \omega_f \Gamma_f} \qquad (2.13)$$

which is of order $\Gamma_Q^2/\omega_f\Gamma_f$. The corresponding value of the critical intensity I_c and numerical values of n_p are discussed in the following section.

C. Critical intensity

In order to relate the threshold condition $n_f = n_c$ to the experimentally controllable quantity, which is the intensity I of the incident radiation in this case, the relation between I and n_f is first derived by equating the energy into the fundamental mode f to the energy out of f by relaxation. In Sec. III it will be shown that near the threshold the increased energy flow from f to the pair has rather important consequences including an increase in the relaxation frequency of the fundamental mode. The usual linear low-intensity value Γ_f of the relaxation frequency is used in the present section in order to obtain the critical value I_c of the intensity.

If the intensity just inside the front face is I_0, the intensity at a distance x into a sample with thickness $\gg 1/\beta$ is $I = I_0 e^{-\beta x} \cong I_0 - \beta x I_0$, where β is the absorption coefficient and the approximate equality holds for $\beta x \ll 1$. The rate of energy absorption in the layer of area Ax is $-A(I - I_0) = Ax\beta I$, where $I_0 \cong I$. Equating this rate of energy absorbed by f to the rate of loss by relaxation $\hbar\omega\Gamma_f(n_f - \bar{n}_f) \times Ax/V \cong \hbar\omega\Gamma_f n_f Ax/V$, where V is the volume of the sample, gives

$$I = \hbar\omega n_f \Gamma_f / V\beta. \qquad (2.14)$$

The well-known result for β for polar crystals is[22]

$$\beta = \frac{4\pi Ne^2}{cm_r n_r V} \frac{\omega\omega_f\Gamma_f}{(\omega^2-\omega_f^2)^2+(\omega_f\Gamma_f)^2}, \quad (2.15)$$

where n_r is the index of refraction and N is the number of ion pairs. With $n_f = n_c$ in Eq. (2.14), the critical intensity is

$$I_c = (\hbar\omega n_c\Gamma_f/V\beta)_{\min}. \quad (2.16)$$

The subscript min denotes that the value of the threshold intensity is to be calculated for all possible pairs, and the lowest of these values determines the observed critical intensity I_c. Recall that the intensities I and I_c are internal to the sample, and reflection at the surfaces must be taken into account to obtain the applied values.

There are two resonance factors in the expression (2.16) for I_c. The first is the *laser-resonance factor* in β in Eq. (2.15). The second is the *pair-resonance factor* in n_c appearing in the brackets in Eq. (2.12). The laser-resonance factor is on resonance when the laser frequency ω is tuned to ω_f. The pair-resonance factor is on resonance for the pairs having phonon frequencies $\omega_Q = \frac{1}{2}\omega$. The minimum in Eq. (2.16) usually occurs at the pair resonance $\omega_Q = \frac{1}{2}\omega$; it is likely that the pair of modes with the lowest threshold will have $\omega_Q = \frac{1}{2}\omega$ (since the resonance factor has a minimum there) unless there are no phonons having this frequency, or the coupling of the fundamental phonon to this resonant pair is very small [$S_Q \ll 1$ in Eq. (2.10)] or there are other pairs having small Γ_Q and large coupling.

In order to obtain numerical values of I_c and n_p, the values of the relaxation frequencies Γ_Q and Γ_f are needed. Since the values of Γ_Q for various phonon modes Q are not well known at present, only rough estimates of the values of I_c and n_p can be obtained: For NaCl at room temperature, $\Gamma_f \cong 2\times10^{12}$ sec^{-1}.[20] First assuming that $\Gamma_Q = \Gamma_f$ and that the coupling is strong ($S_Q = 1$) and using $\omega = \omega_f = 2\omega_Q = 3\times10^{13}$ sec^{-1}, $\beta = 10^5$ cm^{-1}, $N/V = 2.2\times10^{22}$ cm^{-3}, $(2\bar{n}_Q+1) = 5.6$, and $p = 4$ in Eqs. (2.13) and (2.16) gives

$$n_p/N = 0.7, \quad I_c = 1.0\times10^9 \text{ W/cm}^2. \quad (2.17)$$

This is a large value of I_c, and in experiments to look for the instability, a small value of I_c is desirable. Thus, smaller values of Γ_f and Γ_Q are needed. For small-k acoustical modes on the lowest-frequency branch at low temperature, Γ_Q is believed to be small.[28,29] A conservative approximation to the lower limit of Γ_Q is 10^9 sec^{-1}, corresponding to a mean free path of order 1 μm. At low temperature, Γ_f also will be smaller, say a factor of 5 smaller than at room temperature. According to Eqs. (2.16), (2.13), and (2.15) on resonance, $I_c \sim \Gamma_Q^2\Gamma_f^2$ and $n_p \sim \Gamma_Q^2$. Thus, at low temperature,

$$n_p/N = 2\times10^{-7}, \quad I_c = 10 \text{ W/cm}^2. \quad (2.18)$$

It should be emphasized that the value of I_c is sensitive to the value of Γ_Q, and it may not be possible to achieve such a low threshold.

On the other hand, it has already been pointed out[28,29] that it is conceivable that an anomalously low value of $\Gamma_Q = 10^5$ sec^{-1} could be achieved. In this case, the value of I_c would be only 10^{-7} W/cm^2. The results of Secs. II D and V are important in considering such anomalously low values of I_c. In the former, it will be shown that the anomalously low values of I_c are not restricted to crystals without a center of inversion,[9] and in the latter it will be shown that in the usual case in which lasers with pulse lengths of order 10 nsec are used, the steady state is not attained and the threshold intensity is increased drastically above the previously expected value.

D. Effect of unequal frequencies ($\omega_Q \neq \omega_{-Q}$)

In the calculations above it was assumed formally that the fundamental phonon decays into two phonons with equal frequencies. As discussed in Sec. II B, the threshold may be determined by the decay into two modes having unequal frequencies, especially in NaCl-structure crystals.

The occupation numbers n_1 and n_2, as well as the relaxation frequencies Γ_1 and Γ_2 are now assumed to be unequal in general. The balance of power into the pair of modes from the fundamental against the power out of the pair must be considered separately for the individual modes. Following the reasoning of Sec. II B, we find

$$C[n_f(n_1+1)(n_2+1) - (n_f+1)n_1n_2] - \Gamma_1(n_1-\bar{n}_1) = 0,$$
$$C[n_f(n_1+1)(n_2+1) - (n_f+1)n_1n_2] - \Gamma_2(n_2-\bar{n}_2) = 0.$$

The coupled algebraic equation can easily be solved by substitution, which gives

$$n_1 = A\{\operatorname{sgn}A[1 + (\Gamma_2 n_f\bar{n}_2 - \Gamma_1 n_f\bar{n}_1 + \Gamma_2 n_f + \Gamma_1\Gamma_2\bar{n}_1C^{-1})/\Gamma_1A^2]^{1/2} - 1\} \quad (2.19)$$

and

$$n_2 = \bar{n}_2 + (\Gamma_1/\Gamma_2)(n_1-\bar{n}_1), \quad (2.20)$$

where

$$A \equiv [-(\Gamma_1+\Gamma_2)n_f + \Gamma_2\bar{n}_2 - \Gamma_1\bar{n}_1 + \Gamma_1\Gamma_2C^{-1}]/2\Gamma_1.$$

If we now define n_c by

$$n_c = \Gamma_1\Gamma_2/(\Gamma_1+\Gamma_2)C \quad (2.21)$$

it is easily verified that the various limiting behaviors for n_Q found in Sec. II B are still valid for the present case. In particular, the threshold growth at $n_f = n_c$ remains the same. The threshold value n_c in Eq. (2.21) is the same for both modes since n_1 and n_2 are linearly related, as seen in Eq.

(2.20). The values of n_1 and n_2 at the threshold are different in general, of course. Equation (2.21) reduces to Eq. (2.5) if $\Gamma_1 = \Gamma_2$. If one relaxation frequency, $\Gamma_>$, is much greater than the other, $\Gamma_<$, then Eq. (2.21) reduces to $n_c = \Gamma_</C$. Thus the equal frequency approximation employed previously introduces no serious error in either qualitative or quantitative description of the threshold behavior if Γ_Q is interpreted as Γ_1 for the case of $\Gamma_1 = \Gamma_2$ or as the lesser of $2\Gamma_1$ and $2\Gamma_2$ for the case of $\Gamma_1 \gg \Gamma_2$ or $\Gamma_2 \gg \Gamma_1$.

This result that the threshold can be low if *either* mode is long lived (Γ_Q small) is important. In the absence of the analysis above, it might have been guessed incorrectly that the phonon having the shorter lifetime would control the threshold or that one mode might go unstable before the other. The suggestion[28,29] that the phonons on the lowest acoustical branch may have anomalously long lifetimes at low temperature implies that the value of I_c may be anomalously low. Since a selection rule[23-26] prevents both phonons of the pair from being on this lowest branch in crystals with a center of inversion (such as NaCl-structure crystals), it was previously believed that such crystals would not have the anomalously low values of I_c.[9] The present result, that the relaxation frequency Γ_Q that determines the value of I_c is equal to $2\Gamma_<$ when one value $\Gamma_<$ is much less than the other, shows that the lack of a center of inversion is not required.

E. Higher-order two-output-phonon processes

As mentioned in the previous section, the two-phonon processes arising from the cubic anharmonic terms in NaCl-structure materials are subject to rather stringent selection rules[23-26] and quasiselection rules.[27] This is expressed mathematically by the smallness of the factor S_Q in the transition matrix element of Eq. (2.10). By virtue of Eq. (2.13), the critical intensity is increased when S_Q is small, a reasonable result on physical grounds. Since for higher-order processes such as the creation of two phonons from the annihilation of two fundamental phonons [Fig. 3(a)] or that of one fundamental phonon and one other thermal phonon [Fig. 3(b)] the selection rules are more relaxed, it is of interest to examine whether these processes lead to parametric excitation and if so, whether the threshold condition is lowered from the previous first-order case.

Both processes (a) and (b) arise from the fourth-order term of the anharmonic potential $\Gamma_{Q_1Q_2Q_3Q_4}$, which contains a selection-rule-related factor α_3.[30] Process (a) is analogous to the second-order Suhl instability that is responsible for the premature saturation of the main resonance in the ferromagnetic case. The instability condition can be found in exactly the same way as in Sec. II B, and, within the equal frequency approximation, it is

$$I_{c'} = \left(\frac{\hbar c m_r n_r [(\omega^2 - \omega_f^2)^2 + (\omega_f \Gamma_f)^2]}{4\pi N e^2 \omega_f} n_{c'} \right)_{\min} \qquad (2.22)$$

with

$$n_{c'} = \Gamma_{Q'} / |V_{f f Q' -Q'}|$$

where the prime distinguishes the output phonons in Fig. 3 from those of Fig. 1. One readily obtains the ratio of the critical intensities for second- and first-order instabilities as

$$\frac{I_c(\text{2nd order})}{I_c(\text{1st order})} = \left(\frac{2\Gamma_{Q'}}{\hbar \Gamma_Q^2} \right) \left(\frac{|3! V_{f Q -Q}|^2}{|4! V_{f f Q' -Q'}|} \right) . \qquad (2.23)$$

The value of the ratio in Eq. (2.23) can be estimated as follows: For a crystal with two types of ions with masses $m_>$ and $m_<$ ($m_> > m_<$), the vertex coefficients in Eq. (2.23) are[30]

$$|V_{f Q -Q}| = \frac{\alpha_2 B}{4\rho(1-2\rho)N^{1/2}} \left(\frac{\hbar}{2 m_r m_< \omega \omega_Q \omega_{-Q}} \right)^{1/2} \qquad (2.24)$$

and

$$|V_{f f Q' -Q'}| = \frac{\alpha_3 B}{32\rho^2(1-2\rho)N} \left(\frac{\hbar^2}{m_r m_<^3 a^2 \omega^2 \omega_{Q'} \omega_{-Q'}} \right)^{1/2} , \qquad (2.25)$$

where a is the equilibrium nearest-neighbor separation and α_2 and α_3 are angle factors related to selection rules. For fully allowed transitions the α's are of order unity. The result of (2.23) can be resolved into a product of two factors. The first is the ratio $|\alpha_2|^2/|\alpha_3|$, which has to do with the selection rules. The second,

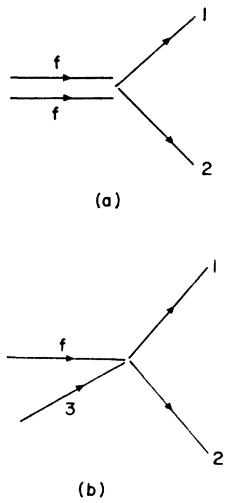

FIG. 3. High-order two-phonon output processes: (a) annihilation of two fundamental phonons, and (b) annihilation of one fundamental phonon and one thermal phonon.

$$8Ba\Gamma_{Q'}/(1-2\rho)m_{\zeta}^{1/2}m_{r}^{1/2}\omega_f\Gamma_Q^2 ,$$

is a dynamical factor and is estimated to be about 1.2×10^3 in NaCl. In obtaining the latter, we have used $\Gamma_Q \cong 1.85\times10^{11}$ sec^{-1} and $\Gamma_{Q'} \cong 5.56\times10^{12}$ sec^{-1}. In order for Eq. (2.23) to be less than unity, the selection rule factor $|\alpha_2|^2/|\alpha_3|$ must be less than 10^{-3}. It is expected that $|\alpha_3|$ will be of order unity, since there is no selection rule and no reason to expect that there are quasiselection rules for this four-phonon vertex. Thus, if the quasiselection rules on α_2 should make $|\alpha_2|^2 < 10^{-3}$ for all potentially unstable pairs, there still would be an instability as a result of the higher-order process.

By proceeding in the same way, one can study the process illustrated in Fig. 3(b). It can be easily demonstrated that such a process is characterized by essentially linear increase of final phonon occupation as n_f increases and hence no threshold occurs. In passing, also note that the two-phonon difference process (two phonons annihilated and one created) does not have a parametric instability.

F. Anharmonic interaction versus high-order dipole moment

The process discussed in Secs. II A–II E is the absorption of radiation by the fundamental mode (driven off resonance in general), which splits into two phonons as a result of the anharmonic interaction. The same end result, that is the absorption of radiation and the creation of two phonons, can result from the Lax-Burstein interaction involving higher-order dipole moments.[25] In this latter process, the photon splits into two phonons directly, with no intermediate state. The Lax-Burstein mechanism usually is considered to be weaker than the anharmonic-potential mechanism (although there is still debate on this point). Since this implies less energy into the potentially unstable pair of phonons, it is expected that the threshold is great for the group-IV semiconductors, diamond, silicon, and germanium, in which the anharmonic-potential mechanism is inoperative. The following simple estimate indicates that this is indeed the case.

The preceding analysis for instability threshold may be used provided one makes the formal replacements of n_f by the number of photons n_p and $|3!\,V_{f12}|^2$ by the square of the new vertex, $|V_p|^2$. The resulting threshold value of the photon occupation number is

$$n_{pc} = \Gamma_Q^2/2|V_p|^2 . \tag{2.26}$$

The value of $|V_p|^2$ can be estimated from the known values of β as follows. First, β is related to the photon relaxation frequency Γ_p, then Γ_p is related to $|V_p|^2$. The time rate of decrease of intensity on passing through a slab of material with absorption coefficient β is

$$\frac{dI}{dt} \simeq \frac{-c\beta I}{\mathrm{Re}n(\omega)} = \frac{-c^2\beta\hbar\omega n_p}{V[\mathrm{Re}n(\omega)]^2} , \tag{2.27}$$

where $\mathrm{Re}n(\omega)$ is the real part of the refractive index. Differentiating $I = \hbar\omega n_p c/\mathrm{Re}n(\omega)V$ directly and assuming linear relaxation gives

$$\frac{dI}{dt} = \frac{-c\hbar\omega\Gamma_p n_p}{V\mathrm{Re}n(\omega)} . \tag{2.28}$$

Equating (2.27) and (2.28) gives the simple relation

$$\beta = \mathrm{Re}n(\omega)\Gamma_p/c . \tag{2.29}$$

The relaxation frequency Γ_p can be calculated assuming interaction V_p, and is given by

$$\Gamma_p = \pi\sum_Q |V_p|^2\delta(\omega - 2\omega_Q)(2\bar{n}_Q + 1)$$

which upon converting into an integral in $\vec{k}$ space, neglecting angular dependence of the integral, and assuming a Debye frequency spectrum with maximum frequency ω_{mx} is approximately

$$\Gamma_p \cong 72\pi N|V_p|^2(2n_{\omega_k}+1)\omega_k^2/\omega_{mx}^3 . \tag{2.30}$$

Equations (2.26), (2.29), and (2.30) lead to

$$\frac{n_{pc}}{N} = \frac{36\pi\omega_k^2\Gamma_Q^2\,\mathrm{Re}n(\omega)}{c\beta\omega_{mx}^3}(2\bar{n}_Q + 1) . \tag{2.31}$$

For $\omega_k/\omega_{mx} \cong 1/2$, $\Gamma_Q/\omega_{mx} = 1/50$, $\omega_{mx} \cong 10^{14}$ sec^{-1}, $\beta = 10$ cm^{-1}, $2\bar{n}_Q + 1 \cong 1$, and $\mathrm{Re}n(\omega_f) = 7$, Eq. (2.31) gives $n_c/N \cong 50$ or $I_c = \hbar\omega n_c c/V\mathrm{Re}n(\omega) \cong 10^{19}$ W/cm^2, which illustrates the great magnitude of the threshold intensity for the Lax-Burstein mechanism.

III. POWER ABSORPTION AND ENHANCED RELAXATION OF THE FUNDAMENTAL MODE

In the limit of $n_f \ll n_c$, the steady-state power out of the fundamental mode is simply $\hbar\omega\Gamma_f n_f$ for $n_f \gg \bar{n}_f$, where Γ_f is the usual linear (low intensity) relaxation frequency. As the intensity is increased and n_f approaches n_c, this steady-state power increases, becoming many orders of magnitude greater than the linear value $\hbar\omega\Gamma_f n_f$ in the formal limit of $n_f \cong n_c$. This increased absorption is a result of the pair-mode occupation numbers n_Q increasing above their thermal equilibrium values caused by the great power flow into the pairs from the fundamental mode. A convenient measure of the increased power flow is the generalized relaxation frequency $\tilde{\Gamma}_f$ defined by the relation

$$\frac{dn_f}{dt} \cong -\tilde{\Gamma}_f n_f , \tag{3.1}$$

again for $n_f \gg \bar{n}_f$. An expression for $\tilde{\Gamma}_f$ will be derived in Sec. III B, and $\tilde{\Gamma}_f$ will be used in the discussion of several effects in Secs. III C, III D, and IV A.

A. Energy flow into a single pair

It will now be shown that the value of the contribution $\tilde{\Gamma}_{f1}$ to $\tilde{\Gamma}_f$ from a single pair, is negligibly small for $n_f \leqq n_c$, while $\tilde{\Gamma}_{f1}/\Gamma_f = 1$ for $n_f = 2n_c$. Consider the power into a single pair of modes from the fundamental mode. In equilibrium, this power is equal to the power out of the pair by relaxation:

$$\left(\frac{d\hbar\omega n_Q}{dt}\right)_{\text{pump}} = \hbar\omega\Gamma_Q(n_Q - \bar{n}_Q) \ . \tag{3.2}$$

The power out of the fundamental mode by linear relaxation is, with $n_f \gg \bar{n}_f$,

$$\left(\frac{d\hbar\omega n_f}{dt}\right)_{\text{relax}} = \hbar\omega\Gamma_f n_f \ . \tag{3.3}$$

For $n_f \leqq n_c$, $n_Q \leqq [n_c(2\bar{n}_Q + 1)]^{1/2}$, and the power (3.2) out of the fundamental mode f to the *single pair* is much less than the power (3.3) out of f by linear relaxation, since $\Gamma_f \gtrsim \Gamma_Q$ usually is satisfied.

Before considering the effect of the *large number* of modes into which f is coupled, note that as n_f is increased above n_c, the value of n_Q in (3.2) increases rapidly: For $n_f > n_c + \epsilon$, (3.3) and (2.8d) give $d\hbar\omega n_Q/dt = \hbar\omega\Gamma_Q(n_f - n_c)$. When $n_f = 2n_c$, the value of n_Q is $2n_c$, and for $\Gamma_f \cong \Gamma_Q$, (3.2) and (3.3) show that the power into the single pair is equal to the total linear-relaxation power out of n_f. This is equivalent to the previous statement $\tilde{\Gamma}_{f1}/\Gamma_f \cong 1$ for $n_f = 2n_c$. Thus, the parametric excitation of many pairs is potentially an extremely strong sink for removing energy from the fundamental mode. This fact is important in the limiting of the value of n_f at a finite value, as discussed in Sec. IV A.

B. Sum over all pairs; dependence of $\tilde{\Gamma}_f$ on n_f

Since there are an enormous number of modes into which the fundamental mode could put energy, it is possible that summing Eq. (2.2) over all pairs could give a number greater than the total linear-relaxation values of $\Gamma_f n_f$ even when the single-pair value in (2.2) is negligible. The following calculation, even though highly simplified, clearly illustrates that this is indeed the case. Summing Eq. (2.2) over pairs and using Eq. (2.1) gives

$$\frac{dn_f}{dt} = -\sum_Q \pi |3!\, V_{fQ-Q}|^2 \delta(\tilde{\omega})[(2n_Q + 1)n_f - n_Q^2] \ . \tag{3.4}$$

Setting $n_Q = \bar{n}_Q$ and using $(2\bar{n}_Q + 1)\bar{n}_f - \bar{n}_Q^2 = 0$ reduces Eq. (3.4) to

$$\frac{dn_f}{dt} = -\Gamma_f(n_f - \bar{n}_f) \ ,$$

where

$$\Gamma_f = \sum_Q \pi |3!\, V_{fQ-Q}|^2 \delta(\tilde{\omega})(2\bar{n}_Q + 1) \ . \tag{3.5a}$$

At higher power levels the value of n_Q is greater than $\bar{n}_Q$. Then, neglecting n_Q^2 reduces Eq. (3.4) to (3.1) with $\tilde{\Gamma}_f$ given by (3.5a) with $\bar{n}_Q$ replaced by n_Q. From Eq. (2.9)

$$2n_Q + 1 = \frac{2\bar{n}_Q + 1}{1 - n_f/n_c} \ . \tag{3.5b}$$

From this result with n_c given by Eqs. (2.6) and (2.4),

$$(2n_Q + 1)\delta(\tilde{\omega}) = (2\bar{n}_Q + 1)\frac{n_p}{\pi\Gamma_Q}\frac{1}{n_c - n_f} \ , \tag{3.6}$$

where n_p is the value of n_c at $\omega = 2\omega_Q$. From Eqs. (2.4), (2.6), and (2.11),

$$n_p = \Gamma_Q^2/2|3!\, V_{fQ-Q}|^2 \ . \tag{3.7}$$

It is assumed henceforth that n_p is the minimum of n_c; i.e., that the minimum occurs at $\omega = 2\omega_Q$. From Eqs. (2.4), (2.6), and (2.11),

$$\frac{1}{n_c - n_f} = \frac{\pi\Gamma_Q}{n_p(1 - n_f/n_p)^{1/2}} \frac{\omega_Q^2\tilde{\Gamma}_Q}{\pi[(\omega_Q^2 - \frac{1}{4}\omega^2)^2 + \omega_Q^2\tilde{\Gamma}_Q^2]}$$

$$\cong \frac{\pi\Gamma_Q}{2n_p(1 - n_f/n_p)^{1/2}}\delta(\omega_Q - \tfrac{1}{2}\omega) \ , \tag{3.8}$$

where the δ-function representation was used in the approximate equality and $\tilde{\Gamma}_Q^2 \equiv \Gamma_Q^2(1 - n_f/n_p)$. In the second term in $\tilde{\Gamma}_Q^2$, it was assumed that $\omega \cong 2\omega_Q$. Substituting (3.6) and (3.5b) into (3.4), neglecting n_Q^2, and evaluating the trivial integral gives (3.1) with

$$\frac{\tilde{\Gamma}_f}{\Gamma_f} = \frac{1}{(1 - n_f/n_p)^{1/2}} \tag{3.9}$$

for this case of $n_f < n_p - \epsilon$. The result (3.9), which can also be derived starting with

$$\frac{dn_f}{dt} = -2\sum_Q \Gamma_Q(n_Q - \bar{n}_Q) \ , \tag{3.10}$$

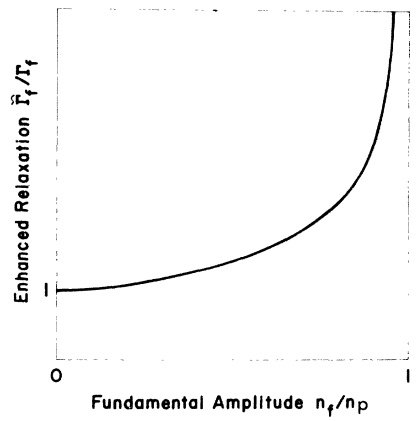

FIG. 4. Enhanced relaxation frequency of the fundamental mode ($n_f < n_p$).

indicates that $\tilde{\Gamma}_f \cong \Gamma_f$ for $n_f \ll n_p$ and $\tilde{\Gamma}_f$ increases to a value much greater than Γ_f as n_f approaches n_p. A plot of Eq. (3.9) is given in Fig. 4.

C. Relation between n_f and I

On the basis of the fact that the relaxation frequency of the fundamental mode is enormously increased at the threshold, one may be tempted to conclude that the power absorption would be increased likewise. This conclusion is erroneous near the laser resonance, since enhanced relaxation of the fundamental mode considered in the previous two sections vastly alters the linear dependence of n_f on the incident intensity I, as will now be shown. Physically, the resonance absorption of a harmonic oscillator is *inversely* proportional to the relaxation frequency. In Sec. III D, the new relation between n_f and I will be used to obtain the behavior of power absorption as a function of I.

In the steady state, the power absorbed is equal to the power $d\hbar\omega n_f/dt$ out of the fundamental mode. Thus, with (3.1),

$$P_{\text{abs}} \cong \hbar\omega\tilde{\Gamma}_f n_f \,. \tag{3.11}$$

Equation (3.11) may be equated to $IV\beta$ (Sec. II C) to yield a relation for n_f in terms of $\tilde{\Gamma}_f$ and I. Using Eqs. (3.9), (3.11), (2.12), (2.15), and (2.16) for the case of laser resonance ($\omega = \omega_f$) and assuming that the minimum in (2.16) occurs at $n_c = n_p$ gives

$$\frac{n_f}{n_p} = \left(\frac{I}{I_c}\right)\left(\frac{\Gamma_f^2}{\tilde{\Gamma}_f^2}\right) = \frac{I_1}{1+I_1}, \quad I_1 \equiv I/I_c \,. \tag{3.12}$$

For low power levels ($I \ll I_c$), $n_f \cong n_p(I/I_c)$, so that n_f increases linearly with the incident intensity. The linear relation is lost with higher intensity, as is evident from Fig. 5. The region of changeover from $n_f \propto I$ to $n_f \cong$ const is not sharp. For n_f to attain a value within a tenth of n_p requires $I = 9I_c$. The value of n_f is limited to values below n_p even for very large values of I. Thus, the simple linearized result (2.9) for n_Q can be used in studying steady-state results. This will not be the case in the time-dependence analysis of Sec. V or, in general, in other applications.

D. Absorbed power and $\tilde{\Gamma}_f/\Gamma_f$ as functions of I

It will be shown that the power absorption spectrum $P_{\text{abs}}(\omega)/I$ is constant for $I \ll I_c$ and decreases in peak amplitude and broadens for I approaching and greater than I_c. First note that (3.9) and (3.12) give

$$\tilde{\Gamma}_f/\Gamma_f = (I_1+1)^{1/2} \,, \tag{3.13}$$

which is unity for $I \ll I_c$ and is equal to $(I/I_c)^{1/2}$ for $I \gg I_c$. The transition between the two limiting behaviors is quite gentle, in contrast to the sharp increase in $\tilde{\Gamma}_f/\Gamma_f$ as a function of n_f/n_p at $n_f/n_p = 1$. (See Fig. 4.)

The power absorption at the laser resonance ($\omega = \omega_f$) is obtained by substituting (3.13) and (3.12) into (3.11), which gives

$$P_{\text{abs}} = \hbar\omega\Gamma_f n_p \frac{I_1}{(1+I_1)^{1/2}} \,. \tag{3.14}$$

From this result (3.14) it is seen that P_{abs} is linear in I for $I \ll I_c$ and increases only as $I^{1/2}$ for $I \gg I_c$. Again, the transition between the two limiting behaviors is smooth. The power-absorption spectrum $P_{\text{abs}}(\omega)/I$ decreases at resonance as I approaches and becomes greater than I_c. This result (3.14) is discussed in Sec. VII.

Since Γ_f, P_{abs}, and T are smoothly varying functions of I, in contrast to the sharp-threshold behavior as functions of n_f, the value of I_c will be referred to as the critical intensity, rather than the threshold intensity.

IV. EFFECTS ABOVE AND NEAR THE THRESHOLD

A. Sticking of n_f

The result, from Sec. III C, that $n_f < n_p$ even for $I \gg I_c$, which will be called the sticking of n_f, is analogous to angle sticking in ferromagnetic resonance.[1] The previous explanation of angle sticking was that the energy flow out of the uniform-precession mode u would be so great when $n_u > n_{uc}$, where n_{uc} is the threshold value of the occupation number n_u of the u mode, that n_u would be reduced to the value n_{uc}. This previous explanation is not strictly correct since the analysis of Sec. III C evinces that the strong flow of energy out of u exists for $n_u < n_{uc}$. Thus, n_u sticks at a value somewhat below n_{uc}, just as n_f sticks at a value below n_p as in Fig. 5. In the following section, the previous explanation of the sticking phenomena is considered briefly.

B. Large value of $\tilde{\Gamma}_f/\Gamma_f$ above the threshold

The fact that the power $\hbar\omega\tilde{\Gamma}_f n_f$ out of the fundamental mode would be extremely large if n_f were

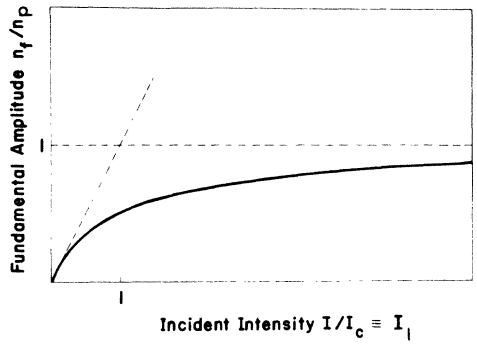

FIG. 5. Dependence of fundamental mode amplitude on incident intensity from Eq. (3.12).

greater than n_p is the key to the previous explanation of angle sticking, as discussed in Sec. IV A. This result is easily explained intuitively as follows: In Sec. III A it was shown that for $n_f = 2n_c$ and $\Gamma_Q = \Gamma_f$ the energy from n_f to a single pair is equal to the total energy out to all pairs by linear relaxation. Thus, $\tilde{\Gamma}_f/\Gamma_f$ is of the order of the total number N_{pairs} of pairs that are above threshold (i.e., have $n_f > n_c$). Since there are of order 10^{23} potentially unstable pairs, the value of $\tilde{\Gamma}_f/\Gamma_f$ is extremely large.

An order-of-magnitude estimate of the size of $\tilde{\Gamma}_f/\Gamma_f$ for the formal case of $n_f > n_p$ is obtained by extending the analysis of Sec. III B to this case. For $n_f > n_p + \epsilon$, Eq. (2.8) is approximately

$$n_Q - \bar{n}_Q \cong 0, \qquad \text{for } n_f < n_c$$
$$\cong 2(n_f - n_c), \quad \text{for } n_f > n_c$$

which, with (3.10) gives

$$\frac{dn_f}{dt} = -4\int_{\omega_-}^{\omega_+} d\omega_Q\, g(\omega_Q)\Gamma_Q(n_f - n_c)\,, \tag{4.1}$$

where ω_+ and ω_- are the positive roots of $n_f = n_c$. With $n_f - n_c$ given by the top equality in (3.8), Eq. (4.1) becomes

$$\frac{dn_f}{dt} = 4n_p\int_{\omega_-}^{\omega_+} d\omega_Q\,\frac{g(\omega_Q)}{\omega_Q^2\Gamma_Q}\left[\omega_Q^2\left|\tilde{\Gamma}_Q^2\right| - (\omega_Q^2 - \tfrac{1}{4}\omega^2)^2\right].$$

When the length $\omega_+ - \omega_- = \Gamma_Q(n_f/n_p - 1)^{1/2}$ of the integration region is short, $g(\omega_Q)/\Gamma_Q$ can be evaluated at $\omega_Q = \frac{1}{2}\omega$. Evaluating the remaining integral gives (3.1) with

$$\frac{\tilde{\Gamma}_f}{\Gamma_f} = \frac{8n_p^2}{3\pi(\bar{n}_Q + \frac{1}{2})n_f}\left(\frac{n_f}{n_p} - 1\right)^{3/2} \tag{4.2}$$

for this case of $n_f > n_p + \epsilon$. Thus, $\tilde{\Gamma}_f/\Gamma_f$ is of order $n_p/(\bar{n}_Q + \frac{1}{2}) \gg 1$ for $n_f \cong 2n_p$.

C. Chain instabilities

In some systems, it is conceivable that the occupation number n_Q of the unstable pair could become so great that the phonons coupled to the pair could also be driven to their threshold. This chain of unstable pairs could be extended to more and more pairs, as illustrated schematically in Fig. 6.

The method developed for deriving the threshold condition enables us to argue that chain process does not occur in the anharmonic-potential-induced phonon instabilities. For $n_f < n_c$, which is satisfied according to the discussion of amplitude sticking in Sec. IV A, Eq. (2.8) gives

$$n_Q < [n_c(2\bar{n}_Q + 1)]^{1/2}\,. \tag{4.3}$$

For these phonons to induce instabilities of other modes, their number n_Q must reach a value of the order of n_c, a requirement that cannot be fulfilled according to Eq. (4.3). In other systems, a very small density of states at the frequency of the threshold pair would be required in order to have chain process.

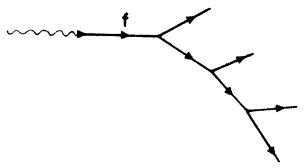

FIG. 6. A chain of parametric processes.

D. Enhanced relaxation of pair modes

In the estimates of critical intensity, we have used the relaxation frequency Γ_Q derived essentially from linear theory. As the instability is approached, the large number of phonons generated interact with one another, leading to further relaxation not accounted for in the linear theory. If this enhanced relaxation were significant, the value of the critical intensity would have to be altered as discussed in Sec. II C. It will now be shown that this is not the case; i.e., the enhanced relaxation is negligible.

Consider the most extreme case, in which n_Q approaches the right-hand side of Eq. (4.3). The dominant mechanism for relaxation is the process in which two of these phonons coalesce to form another phonon under conservation of energy and crystal momenta, as illustrated in Fig. 7. Using the standard quantum-mechanical method, [4] the transition probability of this process was calculated and expressed in the form $dn_Q/dt = -\tilde{\Gamma}_Q n_Q$, from which $\tilde{\Gamma}_Q$ is identified as the enhanced relaxation frequency. Here $\tilde{\Gamma}_Q$ is a function of n_Q. Using the steady-state value of (2.8b), $\tilde{\Gamma}_Q$ is found to be 6×10^6 sec^{-1}, much smaller than the value used for evaluating the critical intensity, so that the enhanced relaxation considered here has little effect in altering the critical intensity.

E. Parametric processes without intermediate states

The sticking of n_f, the nonthreshold behavior of I, and the absence of chain instabilities and enhanced relaxation all are related to the fact that the physical process (Fig. 1) contains an intermediate state, which is the fundamental phonon state in the present case. Other processes, such as the instability of the phonons created in the stimulated Raman process, [7,16] that have intermediate states exhibit similar behavior, as discussed in Sec. II. [17]

By contrast, processes that do not have intermediate states have quite different behavior. For example, in the three-stream plasma instability, no intermediate mode is present and the radiation energy may drive the plasma waves strongly enough

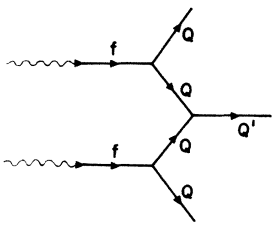

FIG. 7. Enhanced relaxation for phonons Q to phonons Q' when $n_Q \gg \bar{n}_Q$.

to give rise to a chain instability.[31] Similarly, in parallel pumping experiments of ferromagnetic resonance,[4] the rf-field photons convert directly to a pair of magnons without the intervention of uniform precession magnons. In that case the enhanced relaxation of the unstable magnons is indeed significant, and provides a mechanism for additional energy absorption.[32,33]

V. TIME FOR INSTABILITY TO OCCUR

The time τ required for the steady state to be established must be less than the laser pulse length if the steady-state theory is to be applied to experiments using pulsed lasers. It will now be shown that τ is of order Γ_Q, which is sufficiently short under most conditions, but *not* for ultralong-lifetime phonons ($\Gamma_Q < 10^7$–10^8 sec^{-1}). For this latter case, pulses longer than the typical value of 10 ns would be required in order to observe the instability.

The total rate of change of $\eta \equiv n_Q + \frac{1}{2}$ is, from Eqs. (2.3), (2.4), and (2.5), with $-n_Q^2$ negligible,

$$\frac{d\eta}{dt} = \Gamma_Q\left[\bar{\eta} + \eta\left(\frac{n_f}{n_c} - 1\right)\right] . \tag{5.1}$$

The time variation of n_f is, for $n_f \gg \bar{n}_f$

$$\frac{dn_f}{dt} = R - \tilde{\Gamma}_f n_f , \tag{5.2}$$

where $R = V\tilde{\beta}I/\hbar\omega$ is the rate of creation of fundamental phonons by the incident intensity, with $\tilde{\beta}$ given by (2.15) with Γ_f replaced by $\tilde{\Gamma}_f$.

Since $\tilde{\Gamma}_f$ is given as a sum involving the n_Q's, the solution of (5.1) and (5.2) is not trivial. An important practical case is that in which $\Gamma_Q \ll \Gamma_f$. An approximate solution for this case can be obtained as follows. For $n_Q = \bar{n}_Q$, $\tilde{\Gamma}_f$ is equal to the usual low-intensity linear value Γ_f. For all η equal to the steady-state values $\bar{\eta}/(1 - n_{fss}/n_c)$ from (3.5b), where n_{fss} is the steady-state value of n_f, $\tilde{\Gamma}_f$ is equal to the steady-state value $\tilde{\Gamma}_{fss} = \Gamma_f/(1 - n_{fss}/n_p)^{1/2}$ from Eq. (3.9). If the time constant for the approach of η to its steady-state value is denoted by τ, then $\tilde{\Gamma}_f \cong \Gamma_f$ for $t \ll \tau$, and $\tilde{\Gamma}_f \cong \tilde{\Gamma}_{fss}$ for $t \gg \tau$. For the case under consideration, it will be shown that $\tilde{\Gamma}_f$ in (5.2) is slowly varying; that is, $\tau \gg 1/\Gamma_f$. Thus, with $\tilde{\Gamma}_f$ formally considered to be a constant in Eq. (5.2), the solution is

$$n_f \cong \frac{R}{\tilde{\Gamma}_f}\left(1 - e^{-\tilde{\Gamma}_f t}\right) , \tag{5.3}$$

which reduces to

$$n_f = R/\tilde{\Gamma}_f = VI\tilde{\beta}/\tilde{\Gamma}_f\hbar\omega \tag{5.4}$$

for $t \gtrsim (\tilde{\Gamma}_f)^{-1}_{t=0} = \Gamma_f^{-1}$. For still greater times, n_f decreases slowly as $\tilde{\Gamma}_f$ increases, as illustrated schematically in Fig. 8. At the laser resonance ($\omega = \omega_f$), Eq. (5.4) gives

$$\frac{n_f}{n_p} = \frac{I}{I_c}\left(\frac{\Gamma_f}{\tilde{\Gamma}_f}\right)^2 . \tag{5.5}$$

Now $\tilde{\Gamma}_f$ is a function of a sum over Q's. In the spirit of Eqs. (3.9) and (3.5b), we formally assume that

$$(\Gamma_f/\tilde{\Gamma}_f)^2 \cong \bar{\eta}/\eta , \tag{5.6}$$

which is correct at $t = 0$ ($\tilde{\Gamma}_f = \Gamma_f$ and $\eta = \bar{\eta}$) and in the steady state [Eqs. (3.9) and (3.5b)].

Substituting Eqs. (5.6) and (5.5) into (5.1) gives

$$\frac{d\eta}{dt} \cong \Gamma_Q\left[\bar{\eta}\left(\frac{1+I}{I_c}\right) - \eta\right] ,$$

which shows that η increases exponentially to the steady-state value $\eta_{ss} = \bar{\eta}(1 + I/I_c)$ [in agreement with Eqs. (3.5b) and (3.12)] with time constant

$$\tau = 1/\Gamma_Q . \tag{5.7}$$

In passing, it is mentioned that it can be shown rigorously from (5.1) that

$$\tau \geq \Gamma_Q^{-1}(I_c/I)\ln[I/I_c + I_c(I + I_c)^{-1}] .$$

The proof involves the inequality

$$\frac{d\eta}{dt} \leq \Gamma_Q\left(\bar{\eta} + \frac{\eta n_f}{n_c}\right) \leq \Gamma_Q\left[\bar{\eta} + \eta\left(\frac{n_f}{n_c}\right)_{t=0}\right] = \Gamma_Q\left(\bar{\eta} + \frac{\eta I}{I_c}\right) .$$

For a typical value of $\Gamma_Q = 10^{12}$ sec^{-1}, Eq. (5.7) gives $\tau \cong 10^{-12}$ sec, which is short with respect to

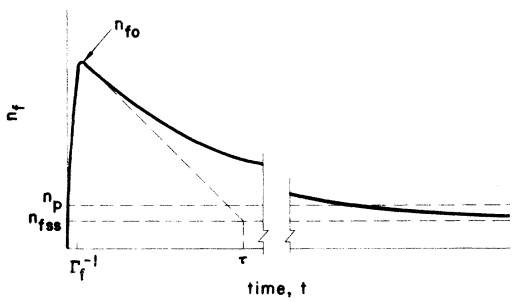

FIG. 8. Schematic illustration of the time dependence of the amplitude n_f of the fundamental mode.

nanosecond pulses, so that the steady-state solution applies. For $\Gamma_Q^{-1} \gtrsim 10^{-8}$ sec, the steady state is not attained in a 10 nsec pulse. In this case, Eq. (5.1) gives $\eta \cong \bar{\eta}$, that is, $n_Q \cong \bar{n}_Q$. Thus $\tilde{\Gamma}_f \cong \Gamma_f$, and the effects of the parametric instability are not observed.

VI. INSTABILITY AT HIGH FREQUENCIES

The effect of phonon instabilities on infrared absorption in the case in which the frequency of the external radiation is high, say, about 3–8 times the reststrahl frequency of the crystal, is of considerable practical interest. Two energy-absorption mechanisms, with the fundamental phonon driven off resonance in both cases, will be considered. In the first case, the fundamental phonon decays into two phonons that are off resonance ($\omega_1 + \omega_2 \neq \omega$). In the second case, the fundamental phonon decays into a sufficient number of phonons to allow phonon resonance to occur ($\omega_1 + \omega_2 + \cdots + \omega_m = \omega$).

A. Two-phonon instability off resonance

This can be considered as a special case of the two-phonon instability discussed in Sec. II, in which the δ function in Eq. (2.11) is far off resonance. For this case Eq. (2.12) reduces to

$$\frac{n_c}{N} = \frac{p(2\bar{n}_Q + 1)(\omega^2 - 4\omega_Q^2)^2}{16 S_Q \omega \omega_Q \omega_f \Gamma_f} . \tag{6.1}$$

With $p = 4$, $(2n_Q + 1) = 5.6$, $\omega = 1.8 \times 10^{14}$ sec^{-1}, $\omega_f = 2\omega_Q = 3 \times 10^{13}$ sec^{-1}, $S_Q = 1$, $N/V = 2.2 \times 10^{22}$ cm^{-3}, $\beta = 5 \times 10^{-4}$ cm^{-1}, and $\Gamma_f = 2 \times 10^{12}$ sec^{-1}, Eqs. (6.1) and (2.16) give

$$n_c/N = 9 \times 10^4, \quad I_c = 1.4 \times 10^{23}\ \mathrm{W/cm^2}, \tag{6.2}$$

which is many orders of magnitude greater than the corresponding critical-intensity values at resonance and is much greater than the avalanche-breakdown value of $\sim 10^{10}$ W/cm^2.[10,13] Thus, the nonlinear absorption by this process is negligible in the high-frequency multiphonon region. This is not surprising since less energy is put into the pair of phonons when they are driven in the wings of their absorption curves than when driven on resonance.

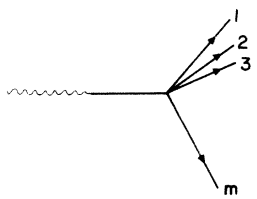

FIG. 9. m-phonon processes.

B. m-phonon instabilities

The second mechanism leading to nonlinear energy absorption at high frequency is the multiphonon process in which a fundamental phonon is annihilated and m phonons are created (Fig. 9). It will now be shown that for sufficiently intense external radiation a parametric instability can set in, as in the previous process.

Again using the general relaxation of power balance gives

$$\left(\frac{dn_i}{dt}\right)_{\mathrm{pump}} + \left(\frac{dn_i}{dt}\right)_{\mathrm{relax}} = 0, \quad i = 1, 2, \ldots, m . \tag{6.3}$$

Proceeding as in Sec. II B yields

$$C^{(m)}[n_f(n_1+1)(n_2+1)\cdots(n_m+1) - (n_f+1)n_1 n_2 \cdots n_m] - \Gamma_i(n_i - \bar{n}_i) = 0 , \tag{6.4}$$

where

$$C^{(m)} = 2\pi |(m+1)!\, V_{f\,12\ldots m}|^2 \times \delta(\omega - \omega_1 - \omega_2 - \cdots - \omega_m) . \tag{6.5}$$

In the present general case, the advantages of using the energy balance method over the equation-of-motion method become even greater than in the case of $m = 2$. The present method yields a single m-order algebraic equation, while the equation-of-motion method leads to m coupled nonlinear differential equations, the solution to which is not easily found.

Since high-order multiphonon processes are subject to much less stringent selection rules than two-phonon processes are, a reasonable first approximation is to assume that the m phonons created have equal frequencies. With this approximation, the set of m equations (6.4) are reduced to the m-order algebraic equation:

$$C^{(m)}[n_f(n_Q+1)^m - (n_f+1)n_Q^m] - \Gamma(n_Q - \bar{n}_Q) = 0 . \tag{6.6}$$

Here n_Q and Γ_Q refer to the occupation number and relaxation frequency, respectively, of a final phonon. The δ function in $C^{(m)}$ will subsequently be approximated, at resonance, by

$$\delta(\omega - \omega_1 - \omega_2 - \cdots - \omega_m) \to 2/m\pi\Gamma_Q . \tag{6.7}$$

It is more expedient to solve for n_f in terms of n_Q than vice versa, which gives

$$n_f = \frac{n^m + \Gamma_Q(n_Q - \bar{n}_Q)/C^{(m)}}{(n_Q+1)^m - n_Q^m} .$$

For n_Q slightly greater than $\bar{n}_Q$, n_f is a sharply increasing function of n_Q until it attains its maximum. This local maximum, denoted by n_c, may be obtained approximately by satisfying the dual conditions that (6.6) yields only one root and that n_Q is small. It is found that, for $m > 2$,

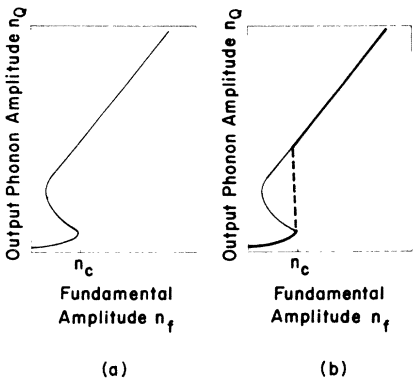

FIG. 10. Parametric excitation of m phonons. (a) Schematic illustration of the approximate steady-state solution to energy balance equation. In (b) the heavy dashed line shows the actual growth path of the final mode as the incident radiation power increases.

$$n_c \cong \Gamma_Q / C^{(m)}(m + b\bar{n}_Q)\{[1 + (2b - m^2)/(m + b\bar{n}_Q)]^{1/2} + 1\}\,, \tag{6.8}$$

where $b = m(m-1)$. Beyond this maximum, n_f as a function of n_Q decreases until $n_Q^{m-1} \cong \Gamma_Q / C^{(m)}$. It then approaches the asymptotic value $n_f \cong n_Q/m$. These features are exhibited in Fig. 10(a).

From Fig. 10(a) it will be noted that for a given value of $n_f (< n_c)$ the occupation number n_Q in the multiphonon region may be multivalued, corresponding to the different branches in the figure. The actual value of n_Q depends on the stability of the solution on a given branch in the presence of fluctuations in the values of n_Q away from the steady-state solution. It is not difficult to demonstrate that all three branches are stable against even extremely large fluctuations, as long as $n_f < n_c$. For $n_f > n_c$, there is only one solution. This behavior indicates that the final modes remain on the lowest branch until the fundamental mode is excited to a value n_c. For greater values of n_f, n_Q increases to the higher-branch value. The value of n_c can therefore be identified as the threshold for m-phonon parametric instability. The actual growth pattern is shown schematically as the heavy curve in Fig. 10(b). The growth from the bottom to the top branch, represented by the heavy dashed vertical line, is not under equilibrium condition since the values in that part of the curve are not steady-state solutions.

Using Eq. (2.16) with n_c replaced by Eq. (6.8), together with Eqs. (6.5) and (6.7), we obtain the following numerical estimates:

$$m = 3, \quad n_c = 0.61N^2, \qquad I_c = 3.9\times10^{13}N \text{ W/cm}^2$$
$$m = 4, \quad n_c = 14N^3, \qquad I_c = 6.5\times10^{15}N^2 \text{ W/cm}^2$$
$$m = 5, \quad n_c = 1.3\times10^{6}N^4, \qquad I_c = 1.4\times10^{21}N^3 \text{ W/cm}^2.$$

In obtaining these estimates, we have not accounted for the limitation due to selection rules so that the actual values are even greater than indicated. For a sample of any reasonable size, the critical intensities in all cases far exceed that required for avalanche breakdown, thus multiphonon instabilities will not be observed.

VII. SUGGESTED EXPERIMENTS

In the preceding section the possibility of parametrically exciting phonons was considered for a wide range of infrared frequencies. The analysis shows that in the higher-frequency region, parametric processes, though possible in principle, have large thresholds I_c so that other nonlinear processes, such as avalanche breakdown, would set in first. In the case of two-phonon excitation, however, the parametric instability should be observable. Of all the possible absorption experiments, consider one of the transmission type. It is necessary to use a sample of thickness no greater than a fraction of a micron, this small thickness being necessary to allow some transmission near the laser resonance.

According to Eq. (2.18), of the order of 10 W/cm^2 are required. For NaCl, with $\lambda_f \cong 60$ μm, and two times diffraction-limited spot of 120 μm diameter, the area is $\sim 10^{-4}$ cm^2, corresponding to a power of $\sim 10^{-3}$ W. In practice, several-orders-of-magnitude-greater power may be required. Since tunable sources with this power are not currently available, a fixed frequency laser must be used. For example, H_2S with lines at 60.3 μm[34] could be used with NaCl. A low-power spectroscopic measurement of the absorption as a function of ω could be made to determine the position of the NaCl absorption curve with respect to the laser frequencies.

The transmission would be measured as a function of the incident power. A noticeable change [increase at resonance—see Eq. (2.15) with $\Gamma_f \to \tilde{\Gamma}_f$] should occur as I approaches I_c, corresponding to the increase in $\tilde{\Gamma}_f$.

For a thin film of crystal of thickness d, the transmission coefficient T_r is given by[20]

$$T_r \cong 1 - \omega d c^{-1} \mathrm{Im}\epsilon(\omega), \quad d \ll \lambda/2\pi \tag{7.1}$$

where $\mathrm{Im}\epsilon(\omega)$ is the imaginary part of the dielectric function $\epsilon(\omega)$. At $\omega = \omega_f$, Eq. (7.1) gives

$$1 - T_r \cong \omega_0^2 d c^{-1}(\epsilon_0 - \epsilon_\infty)\tilde{\Gamma}_f^{-1} = (1 - T_r)_{\text{lin}}(I/I_c + 1)^{-1/2}\,. \tag{7.2}$$

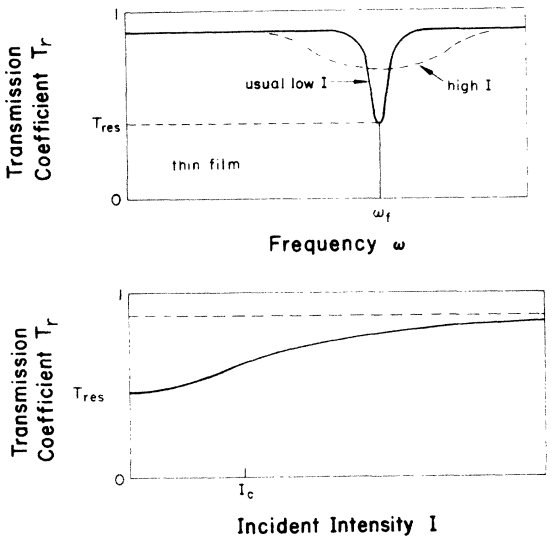

FIG. 11. Spectral transmittance of a thin film schematically illustrating the broadening of the resonance at high values of incident intensity. The bottom curve was sketched using Eq. (3.14).

In the second equality, the result (3.13) for $\tilde{\Gamma}_f$ was used. The subscript "lin" denotes that $1 - T_r$ is evaluated at $\tilde{\Gamma}_f = \Gamma_f$. By correlating this dependence of $1 - T_r$ on I with the experimental results, parametric processes may be verified. In particular, according to Eq. (7.2), the transmission coefficient of a thin film driven parametrically at resonance should increase as I increases, while T_r decreases with increasing I away from resonance. This behavior is analogous to that observed in the premature saturation of the main resonance in the Suhl-Bloch-Bloembergen ferromagnetic instability. Figure 11 illustrates the change in transmission with increasing intensity.

In principle, the parametric instability could be used to study the relaxation frequencies of various phonon modes as a function of the position of the modes in the Brillouin zone, as has been done for magnons in parallel pumping experiments.[4] However, the results would be more difficult to interpret than in the magnon case since it would be more difficult to determine unambiguously which phonons were going unstable in general.

---

*Research supported by the Advanced Research Projects Agency of the Department of Defense and monitored by the Defense Supply Service-Washington, D.C.

[1]H. Suhl, J. Phys. Chem. Solids 1, 209 (1959).
[2]H. B. Callen, in *Fluctuation, Relaxation and Resonance in Magnetic Systems*, edited by D. ter Haas (Oliver and Boyd, Edinburgh, Scotland, 1962).
[3]R. M. White and M. Sparks, Phys. Rev. 130, 632 (1963).
[4]M. Sparks, *Ferromagnetic Relaxation Theory* (McGraw-Hill, New York, 1964).
[5]S. V. Silin, Zh. Eksp. Teor. Fiz. 48, 1679 (1965) [Sov. Phys.-JETP 21, 1127 (1965)].
[6]D. F. DuBois and M. V. Goldman, Phys. Rev. Lett. 14, 544 (1965).
[7]N. Bloembergen, *Nonlinear Optics* (Benjamin, New York, 1965).
[8]W. H. Louisell, *Coupled Modes and Parametric Electronics* (Wiley, New York, 1960).
[9]R. Orbach, IEEE Trans. Sonics and Ultrasonics 14, 140 (1967).
[10]D. W. Fradin, E. Yablonovitch, and M. Bass, Appl. Opt. (to be published).
[11]N. Bloembergen, Appl. Opt. 12, 661 (1973).
[12]M. Sparks and C. J. Duthler, J. Appl. Phys. 44, 3038 (1973).
[13]L. V. Keldysh, Zh. Eksp. Teor. Fiz. 47, 1945 (1964) [Sov. Phys.-JETP 20, 1307 (1965)]; G. M. Zverev, T. N. Mikhailova, V. A. Pashkov, and N. M. Solov'eva, Zh. Eksp. Teor. Fiz. 53, 1849 (1967) [Sov. Phys.-JETP 26, 1053 (1968)].
[14]S. A. Akhmanov, A. P. Sukhorukov, and R. V. Khokhlov, Usp. Fiz. Nauk 93, 19 (1967) [Sov. Phys.-Usp. 10, 609 (1968)]; M. T. Loy and Y. R. Shen, IEEE J. Quantum Elec. QE-9, 409 (1973).
[15]M. Sparks, J. Appl. Phys. 42, 5029 (1971).
[16]M. Sparks, Phys. Rev. Lett. 32, 450 (1974).
[17]M. Sparks (unpublished).
[18]The processes with the vertex V_Q appearing first and those with the intermediate-state boson being annihilated, then created, must also be considered, of course. Treating these diagrams in second-order perturbation theory and formally replacing $\Gamma_f(\omega^2 - \omega_f^2)^{-2}$ by $\Gamma_f[(\omega^2 - \omega_f^2)^2 + \omega_f^2\Gamma_f^2]^{-1}$ gives the same results as those obtained in the present paper, but affords somewhat less insight into the results and cannot be applied directly to other problems such as stimulated Raman scattering.
[19]The polariton nature of the intermediate state need not be considered explicitly in either the photon or magnon case.
[20]M. Born and K. Huang, *Dynamical Theory of Crystal Lattice* (Oxford U. P., Oxford, England, 1954).
[21]M. Sparks and C. J. Duthler (unpublished).
[22]R. A. Cowley, Adv. Phys. 12, 421 (1963).
[23]E. R. Cowley and R. A. Cowley, Proc. R. Soc. Lond. A287, 259 (1965).
[24]E. R. Cowley, J. Phys. C 5, 1345 (1970).
[25]M. Lax and E. Burstein, Phys. Rev. 97, 39 (1955).
[26]R. Loudon, Phys. Rev. 137, A1784 (1965).
[27]C. J. Duthler and M. Sparks, Phys. Rev. B 9, 830 (1974).
[28]L. A. Vredevoe, Phys. Rev. 140, A930 (1965).
[29]R. Orbach and L. A. Vredevoe, Physics 1, 91 (1964).
[30]M. Sparks and L. J. Sham, Phys. Rev. B 8, 3037 (1973).
[31]H. C. Kim (private communication).
[32]P. Gottlieb and H. Suhl, J. Appl. Phys. 33, 1508 (1962).
[33]J. J. Green and E. Schlomann, J. Appl. Phys. 33S, 1358 (1962).
[34]J. C. Hassler and P. D. Coleman, Appl. Phys. Lett. 14, 135 (1969).